# Portable Visible Spectrophotometer for Glucose Microdroplet Measurements in Digital Microfluidic System

Alzana Armaniar Farhani*, Balkan Khilmi Assakandari†, Anindhita Nayazirly‡,
Akhmadi Surawijaya§, Muhammad Ogin Hasanuddin¶
*Department of Electrical Engineering*
*School of Electrical Engineering and Informatics*
*Institut Teknologi Bandung*
Bandung, Indonesia
*farhanialzana@gmail.com, †balkankhilmi@gmail.com, ‡zirlysukarno@gmail.com, §asurawijaya@itb.ac.id, ¶moginh@itb.ac.id

***Abstract*—We propose a portable visible spectrophotometer with an ability to integrate with a digital microfluidic (DMF) system. An interface which consists of an LCD and a set of buttons allows users to gather and view measurement results in a continous manner. The device had a dimension of 120 x 131 x 207 mm$^3$ with the weight of 0.832 kg. The device measured absorbance in the wavelength range of 400 to 700 nm with a resolution of 0.77 nm. The device was tested by assessing the accuracy and repeatability of the transmission and wavelength measurements, as well as the wavelength resolution. The transmittance error was ±11.22% with ±9.88 nm wavelength error. The device had a transmittance repeatability of ±2.58% and wavelength repeatability of ±0.63 nm.**

***Index Terms*—Spectrophotometry, Droplets, Portable, Digital microfluidics**

## I. Introduction

The clinical diagnosis of metabolic diseases, such as diabetes mellitus, highly depends on the measurement of glucose in body fluids. The number of people suffering from diabetes is rising, and over 1 in 10 adults in the world is affected. By 2045, 780 million people worldwide are predicted to live with diabetes [1]. Diabetes patients are at a higher risk of critical health problems than non-diabetic individuals. As a result, accurate monitoring of blood glucose concentrations in diabetic patients is crucial for real-time diabetes diagnosis.

Currently, various methods detect and measure glucose concentrations. These methods can be broadly grouped into two main categories: enzymatic approaches, such as spectrophotometric assays; and non-enzymatic approaches, such as HPLC systems. While the first group is glucose specific, the latter is broadly adaptable and can be used to detect not only glucose but a wide variety of other carbohydrates as well [2]. However, the spectrophotometric test is becoming a more commonly used method for glucose detection because of its ability to detect in a shorter time and at a lower cost. Spectrophotometric tests utilize the light transmitted or reflected by a sample to perform qualitative and quantitative analysis. For qualitative analysis, the light transmitted by a sample has a unique spectrum based on the atoms or molecules contained in the sample.

Meanwhile, for quantitative analysis, the absorbance level of the sample for a specific wavelength is directly proportional to the concentration of the sample. Glucose spectrophotometry test includes colorimetric measurement methods, namely measurements that involve changing the color of the sample to measure quantities such as absorbance and sample concentration. Various colorimetric methods involving reactions with different enzymes for glucose measurement are the object of research being developed to obtain colorimetric methods that are accurate, sensitive, selective, and inexpensive. There are several enzymes that take glucose as a substrate and turn it into a product or byproduct that can be measured or detected. In particular, the development of spectrophotometric and colorimetric glucose assays has taken advantage of the activities of glucose oxidase and hexokinase enzyme [2]. Several approaches were studied to develop a colorimetric glucose biosensor by using glucose oxidase (GOx) to oxidize glucose to gluconic acid and hydrogen peroxide ($H_2O_2$). In colorimetric assays, studies revealed that the Horseradish Peroxidase (HRP) enzyme could catalyze the reaction of H2O2 and organic substrates such as 3,3',5,5'-tetramethylbenzidine (TMB) to produce visible colors [3].

Microfluidics offer several advantages for glucose analysis, such as reduced sample and reagent consumption, faster analysis, portability, and high compatibility with multiplexing detection means [4], [5]. One application called digital microfluidics (DMF) has a promising potential to operate microdroplets in portable analytical systems. The platform is based on the droplet manipulation using electrowetting-on-dielectric (EWOD) principle which applies electric potential to the control electrodes coated with a hydrophobic dielectric [4]. The DMF system mainly consists of a fluid layer located between the top and bottom plates. Nowadays, DMF technology is commonly used for various processes which include sample preparation and diagnostics [6]. Droplet mixing

allows chemical reactions to be done on chip. An optical detection system needs to be developed in order to measure the absorbance and concentration of a glucose droplet on the DMF chip.

In this study, we present the development of a portable visible spectrophotometer, which is detachable to DMF platforms. It allows the integration with a DMF platform and can be removed if the DMF is needed for other purposes. A light will be emitted through the droplet located on the DMF chip and an array of photodetectors will collect the intensity of incident light. A custom program is used in the system to compute the absorbance and the concentration of the sample droplet. Users can interact with the system using four input buttons and an LCD which displays the result of the measurements.

The spectrophotometer was designed to satisfy several features as follows:

- Concentration measurement of microdroplet samples
- Absorbance measurement of samples based on wavelength characteristic
- Able to work in visible spectrum (400 nm to 700 nm)
- Able to be integrated with a digital microfluidic platform
- The measurement results can be displayed on an LCD and stored
- Portable (should be smaller than 420 x 300 x 180 $mm^3$ and weighs less than 2 kg)

## II. Materials and Methods

### A. System Overview

The proposed system consists of five subsystems which are light source, light sensor, control and processing system, user interface, and power subsystem. Its data flow diagram (DFD) is shown in Fig. 1. The light sensor subsystem is composed of a slit, a monochromator, and an array of photodetector. The source light, which is emitted by a polychromatic light source, will be passed through the sample droplet located on an electrode of a DMF platform. The light which is not absorbed by the droplet will pass through the slit then to a monochromator. The monochromator decomposes the light into monochromatic light to be detected by the photodetector array. Each detector in the array measures the light intensity for a specific wavelength. The measurement readings will be sent to the control subsystem to be computed into absorbance values.

### B. Light Source Subsystem

The light source subsystem's function is to produce polychromatic light as the primary variable to be manipulated and measured by the instrument. This subsystem includes two modules, namely switching circuits and a lamp as the light source. The process in this subsystem begins with receiving a control signal from the control subsystem to the switching circuit. Switching circuit is used to turn the light source on and off. The polychromatic light source will illuminate and produce light with all UV-Vis frequencies within the specification. This light is then passed on to the sample for a certain period.

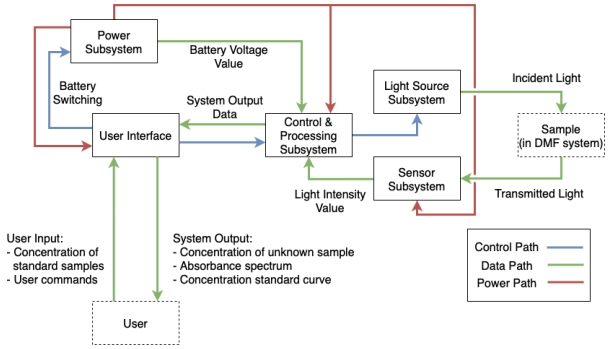


Fig. 1. Level-1 Data Flow Diagram (DFD) of the system

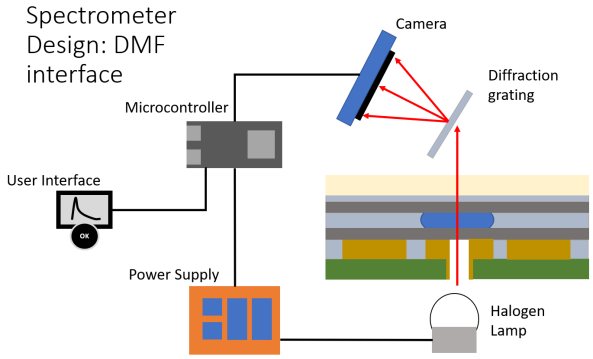


Fig. 2. The main components of the proposed device

### C. Light Sensor Subsystem

The light sensor subsystem functions as a spectrometer that receives polychromatic light beam and outputs light intensities of discrete wavelengths in the form of digital data. Polychromatic light beam enters the sensor subsystem through a hole and gets diffracted by a transmissive diffraction grating as to spatially separate light by its wavelengths. The grating has a groove density of 1200 lines/mm, and the first order of diffraction is used to separate the visible spectrum. The diffracted ray is then recorded by a CMOS image sensor (Arducam MT9M001 Monochrome Camera Module). Different pixel of the image sensor captures the intensity of different wavelengths ranging from 400 nanometer to 700 nanometer formatted into 10-bit unsigned integer. The light sensor subsystem outputs, at maximum, 400 16-bit unsigned integer values, each value representing the light intensity of wavelengths in the visible spectrum range.

### D. Control and Processing Subsystem

The control and processing subsystem consists of control and data processing unit. Other subsystems in the spectrophotometer are controlled by a ESP32-S3-DevkitC-1 microcontroller board (Espressif Systems, China)/ The task of the control unit is to execute the main workflow of the spectrophotometer by a Finite State Machine (FSM). The control subsystem synchronizes other subsystems, such as the light source with the light sensor when measuring light

intensities. Data processing unit's main function is to process data signals for by converting the sensor intensity data into absorbance values. It converts the sensor's intensity data into an absorbance spectrum (spectrum mode) and performs linear regression to calculate the sample concentration according to the standard samples.

C++ programming was used to create the control subsystem program, and the PlatformIO IDE for Microsoft Visual Studio Code was used (VSCode). Control unit's function is to execute the spectrophotometer's processes based on the designed FSM as shown in Fig. 3.

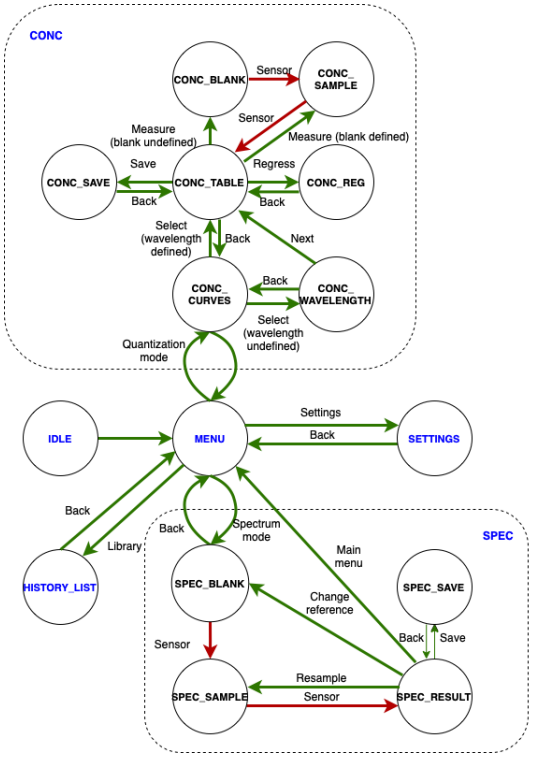


Fig. 3. FSM diagram of the portable visible spectrophotometer

The absorbance $A$ of a particular sample is computed by the Equation (1).

$$A = -\log 10T = \log \frac{I_0}{I} \tag{1}$$

Transmittance $T$ is the percentage of incident radiation that the sample transmits, $I_0$ denotes the intensity of polychromatic light entering the sample, and $I$ denotes the intensity of light leaving the sample; Absorbance is directly proportional to the path length $l$ through the medium and the concentration $c$ of the absorbing substance for monochromatic radiation. Beer-Lambert's law, expressed in Equation (2), serves as the basis for quantitative analyses using both atomic and molecular absorption measurements ($\epsilon$) is the molar attenuation coefficient) [7].

$$A = \epsilon l c \tag{2}$$

Beer-Lambert's law states that the concentration of a dilute solution is directly proportional to its absorbance value. As a result, in the quantization mode, a linear regression is performed to obtain a slope-intercept form linear equation, as follows.

$$A = mc + b \tag{3}$$

where $m$ is the line's slope (gradient) and $b$ is the constant representing the linear equation's y-intercept.

The measurement data are stored on an external SD card that is part of the data processing device. The data for the absorbance spectrum and the calibration curves for the quantization mode are tabulated in a CSV-file format. The interface between the micro-SD card and the control system is provided by a microSD click module (MikroElektronika, Serbia). In order to store calibration values for absorbance measurement and quantization-mode calibration curves, the microcontroller also utilizes its non-volatile memory storage (NVS).

### *E. User Interface Subsystem*

The user interface subsystem plays a role in connecting the system and the users. This can be done by interpreting the commands given by users through the input interface devices and process it into control signals that will be sent to the control subsystem. The subsystem also has a function to display measurement data which include sample concentration values, sample absorbance spectrum, regression curves, menus, and settings. Fig. 4 shows the data flow diagram of the user interface subsystem.

Four push buttons and a power switch are used as the input interface devices. For the display, a 3.5-inch non-touchscreen TFT LCD with ILI9488 driver is used. The configuration of buttons and non-touchscreen LCD is chosen because it fits the users who will use the spectrophotometer using laboratory gloves.

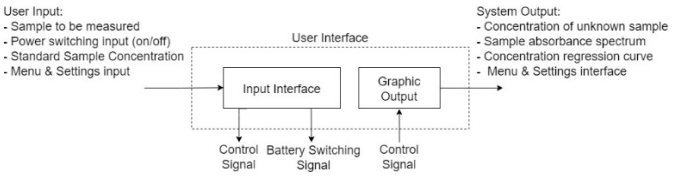


Fig. 4. DFD of the user interface subsystem

### *F. Power Subsystem*

The power subsystem enables the system to be activated by supplying power from the battery to the entire electrical circuit. The battery can be recharged with a 12 V adapter whenever the battery voltage is insufficient. The power subsystem also provides information about the battery voltage value to be displayed to the user.

The power from the adapter is converted into 8.4 V (full capacity) using a charging module when charging is needed.

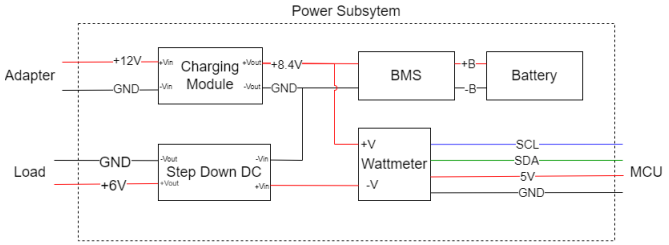


Fig. 5. Schematic of the power subsystem

The power subsystem is activated when the user presses the power button for the first time—allowing the 8.4 V to flow from the battery or the adapter(when charging) to the DC step-down module, giving 6 V output to the microcontroller and other loads. If the battery voltage value is below the threshold or the user presses the power button again, the power supply to the entire circuit will be cut off, and the system will be disabled.

### G. Hardware Assembly

To design the casing and individual parts of the spectrophotometer, we used Autodesk Fusion 360 software. The 3D-printed body consists of the casing, the optical light path, and the lamp holder. Fig. 6 displays internal components of the device. Polylactic acid (PLA) and acrylonitrile butadiene styrene (ABS) filament colored in black were used due to the need of low light reflectance. Electronic parts like printed circuit boards (PCBs) and optical parts were placed inside the main body.

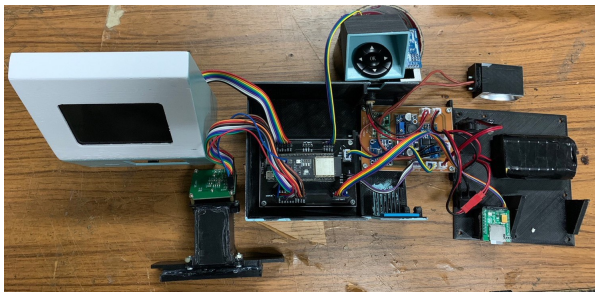

Fig. 6. Overview of the device's internal components

## III. Results and Discussion

### A. Accuracy

Glucose samples were prepared using a glucose assay kit (Glucose (GO) Assay Kit, Sigma-Aldrich [8]) with concentration of 40 µg/ml and 60 µg/ml. The resulting liquid was then placed between two microscope slides spaced 0.5 mm apart to mimic the light path of the DMF cartridge.

Fig. 7 shows the measurement results of the glucose experiment with baseline correction using linear regression. Manual baseline correction was found necessary because of a voltage fluctuation found between blank measurement and sample measurement. Value of 0.155 peak absorbance were detected at 519 nm for 40 µg/ml and 0.079 at 526 nm for 60 µg/ml. Absorbance for the 40 µg/ml sample turned out higher than the 60 µg/ml sample. This result does not fit the absorbance-concentration relation of the Beer-Lambert's law. It was also observed that the 40 µg/ml sample appeared darker for the naked eye. Thus, a retest of the chemical reactions was due.

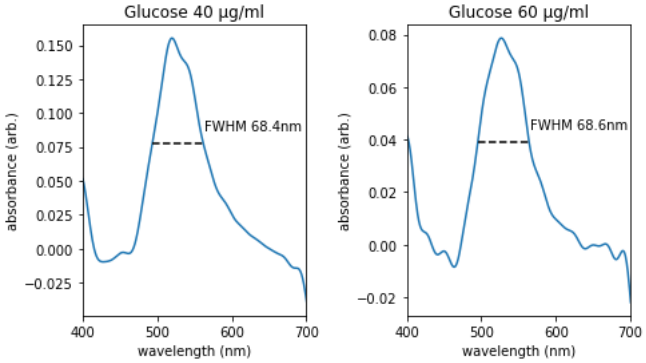


Fig. 7. Glucose absorbance spectrum measurement result, baseline corrected

Aside from glucose, we have tested the spectrophotometer with food dye measurements. Blue (630 nm peak), red (508 nm peak), and yellow (427 nm peak) food dyes were mixed with water. The volume percentages used were 0.033%, 0.040%, 0.050%, and 0.067%. The device's measurements are shown in Fig. 8. The device's measured transmittance spectra was compared to the transmittance spectra from a commercial spectrophotometer (Evolution 220 UV-Visible, Thermo Scientific™). The average transmittance spectrum RMSE obtained was 11.22%. Peak wavelength errors were $+0.99$ nm, $-1.05$ nm, and $+29.71$ nm for blue, red, and yellow dyes respectively.

The biggest error factor for transmittance was the shift in the baseline. The device measured numerous instances of negative absorbance. A negative absorbance is the result of a transmittance higher than 100%. Transmittance is defined as $T = I_{sample}/I_{blank}$, which means the blank intensity readout was lower than the sample intensity readout. In other words, the sensor deemed the blank (water) darker than the sample. This could happen when the intensity from the light source was darker for the blank than the sample. The voltage log confirmed this hypothesis. A blank measurement took longer time than a sample measurement. The longer a measurement took time, the lower the power dropped, hence the lower the intensity became.

The significant increase of the peak wavelength error for the yellow dye was caused by the spectrum response of the system. The yellow dye was evaluated at its peak absorbance wavelength of 427 nm. The pixel spectrum response in 400 nm is 45% the response in 550 nm. Moreover, the lamp emission in 400 nm is 50% the emission in 700 nm. These effeciency drops caused low intensity readouts, which increased resolution and noise in lower wavelengths (400 to 450 nm). Increasing the lamp power was not an option because the heat would damage the plastic structures of the light path.

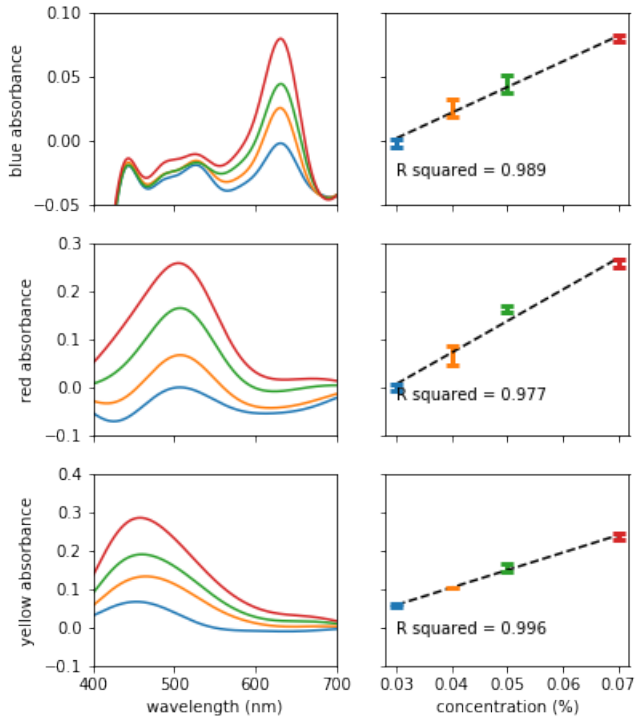


Fig. 8. Dye measurement results

Measurements of the food dye samples were regressed as shown in Fig. 8 to create standard curves. The wavelengths of which the absorbances were measured were the peak absorbances of each dye. An upward trend was found in accordance to the Beer-Lambert's law.

### B. Repeatability

The results of 40 ug/ml glucose transmittance measurements in Fig. 9 for ten iterations show that the average standard deviation at all wavelengths is 2.58% with a maximum deviation of 5.28% and a minimum of 0.87%. As a reference, the standard deviation is also measured at a wavelength of 540 nm, based on the Sigma Aldrich Glucose Assay Kit datasheet. The transmittance's standard deviation at 540 nm is 4.09%.

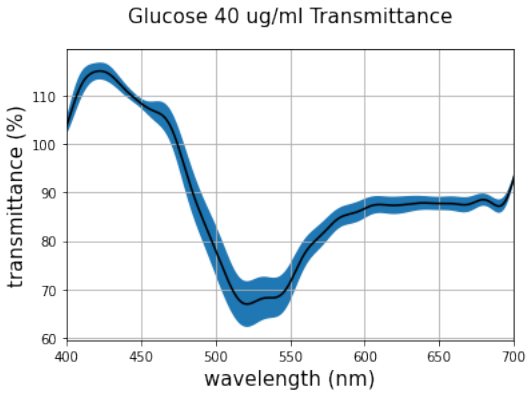


Fig. 9. Glucose 40 ug/ml Transmittance

Based on Fig. 10, out of 10 measurement iterations, the maximum peak wavelength occurs at 521.76 nm, with the minimum peak wavelength at 519.46 nm. On average, the peak wavelength that occurs is 521.07 nm, indicated by a black line on the graph. From this data, the average wavelength standard deviation is at 0.63 nm, with a minimum deviation of 0.69 nm and a maximum deviation of 1.61 nm.

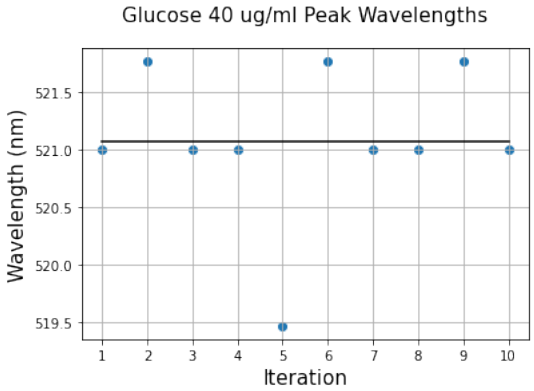


Fig. 10. Glucose 40 ug/ml Peak Wavelengths

The wavelength precision and transmittance of the device were affected by several factors. The first factor was the stability of the internal structure of the product. During the implementation and testing process, it was observed that opening and adjusting the device's case for troubleshooting caused positional shifts of the components. Light pathway obscured by other components could cause light intensity reduction.

From several tests, the treatment of the ITO glass layer (which has been coated with silicon oil and parafilm) also produced a different level of precision. ITO glass should have a holder, for example, a case with a clamp. This way, the light path length is constant. Other than that, the droplet's shape, which tends to be convex at the top, can cause lensing effect [3].

### C. Resolution

Resolution testing is carried out by calculating the resolution of the measurement results stored on an external SD card in the form of a CSV file. The number of pixels needed for the absorbance spectrum measurement, which is obtained from the calibration results, was 297. The absorbance measurement results are stored on an external SD card with a resolution that can be calculated using Equation (4).

$$resolution = \frac{\lambda_{max} - \lambda_{min}}{n_{pixels}} = \frac{(700 - 400)nm}{360} \approx 0.84nm \tag{4}$$

### D. Weight and Size

Weight measurement is done by placing the device on a digital scale which shows the weight is 0.832 kilograms. The final dimension of the spectrophotometer are 120 x 131 x 207

$mm^3$, as shown in Fig. 11 Device's dimensions are affected by the number of components used in the system and the optical configuration used. The sensor's location, diffraction grating, and light source mainly influence the device's height. The battery has a size of 70 x 42 x 21 $mm^3$, which significantly affects the determination of the minimum area of the base. In addition, the button component with a diagonal position uses a large enough area but leaves some empty space.

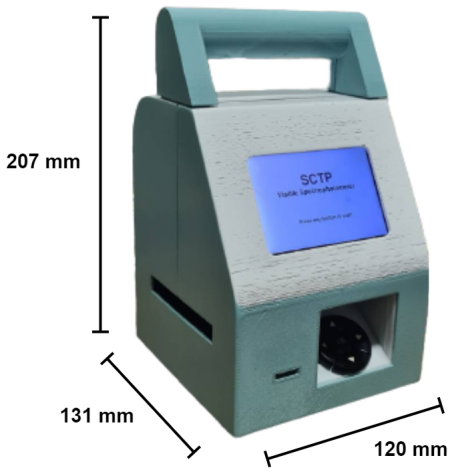


Fig. 11. Device's dimensions

### E. User Interface

The first page of the spectrum-mode measurement instructs the user to insert the blank reference sample into the DMF system. The sample input page, which resembles the blank input page, will be on the next page. A result page with the peak wavelength and absorbance results will show up after the other subsystems have finished measuring absorbance. The user has the option to save the result, return to the main menu, or view the entire spectrum of the absorbance measurement. Fig. 12 illustrates how the result and spectrum page of the absorbance measurement is shown.

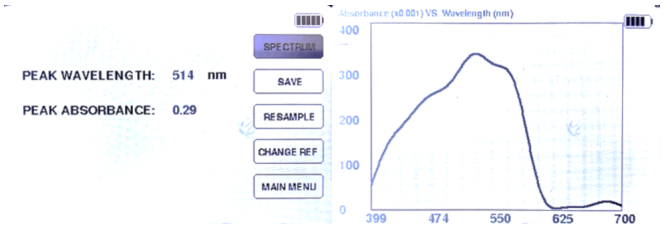


Fig. 12. The display of the result (left) and spectrum (right) page of a spectrum-mode measurement

Quantization-mode measurement starts with a display page that shows the list of saved curves. Users have the option of using, removing, or adding new curve data. The user will get a table page if they select an existing curve. The table consists of concentration and absorbance values of standard samples, as shown in the left side of Fig. 13. By moving the pointer to the desired absorbance (A) cell and clicking the OK physical button, an absorbance measurement for each concentration value should be made. The user will be directed to the blank and sample input page. The user should click the REGRESS button to calculate the concentration of the unknown sample and view the standard curve plot (Fig. 13). There are six curve slots available and each curve can store up to 10 sets of concentration and absorbance values.

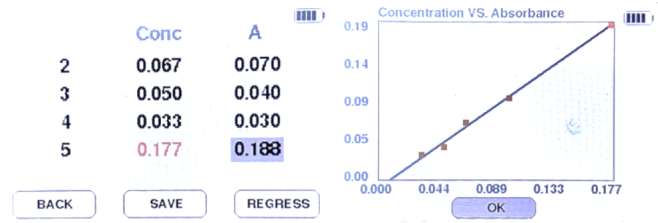


Fig. 13. The display of the table (left) and plot (right) page of a quantization-mode curve

## IV. Conclusions

To support the study of spectrophotometry analysis in DMF platform, we have designed and assembled of a portable visible spectrophotometer that can be integrated with a particular DMF system. Data acquisition, storage, and user experience is made simpler by our developed portable visible spectrophotometer and a user-friendly interface. Measurement's accuracy of red, yellow, and blue food dyes and its repeatability demonstrated good performances in experimental validation versus commercial spectrophotometer (Evolution 220 UV-Visible, Thermo Scientific™). The colorimetric glucose assay (maximum of absorbance at 540 nm) measurements were comparable at certain degree but quite inferior; these issues could be resolved by retesting the colorimetric reactions more thoroughly. Future work will focus on designing a better voltage regulation and heat insulation for the lamp, as well as reducing movable parts from the light path configuration.

## Acknowledgement

The authors thank Dr. Isa Anshori, from Department of Biomedical Engineering, and his research team for assistance with DMF integration and sample preparation. This work was funded by the Department of Electrical Engineering, Institut Teknologi Bandung.

## References

[1] "IDF Diabetes Atlas Tenth edition." [Online]. Available: https://diabetesatlas.org/. [Accessed: 12-Dec-2022].
[2] A. L. Galant, R. C. Kaufman, and J. D. Wilson, "Glucose: Detection and analysis," Food Chemistry, vol. 188, pp. 149–160, 2015.
[3] H. V. Tran et al., "Silver nanoparticles-decorated reduced graphene oxide: A novel peroxidase-like activity nanomaterial for development of a colorimetric glucose biosensor," Arabian Journal of Chemistry, vol. 13, no. 7, pp. 6084–6091, Jul. 2020, doi: 10.1016/j.arabjc.2020.05.008.
[4] Z. Gu, M. L. Wu, B. Y. Yan, H. F. Wang, and C. Kong, "Integrated Digital Microfluidic Platform for Colorimetric Sensing of Nitrite," ACS Omega, vol. 5, no. 19, pp. 11196–11201, May 2020, doi: 10.1021/acsomega.0c01274.

[5] R. B. Fair, A. Khlystov, V. Srinivasan, V. K. Pamula, and K. N. Weaver, "Integrated Chemical/biochemical sample collection, pre-concentration, and analysis on a digital microfluidic lab-on-a-chip platform," SPIE Proceedings, 2004.
[6] S. Huang and R. B. Fair, "Quantitative measurements of inorganic analytes on a digital microfluidics platform," SN Applied Sciences, vol. 1, no. 12, Dec. 2019, doi: 10.1007/s42452-019-1693-8.
[7] D. A. Skoog, F. J. Holler, and S. R. Crouch, Principles of Instrumental Analysis, 7th ed. Cengage Learning, 2016.
[8] B. E. Raabo and T. C. Terkildsen, "On the enzymatic determination of blood glucose," Scandinavian Journal of Clinical and Laboratory Investigation, vol. 12, no. 4, pp. 402–407, 1960.